

# Nonlinear Analysis of CCM Superbuck Converter Using Wigner-Ville Distribution

YUE HU, XIAONA LIU, XUE NI, LIHUA WANG  
Department of Electronic and Information Engineering  
Shandong University of Science and Technology  
No. 579 Qianwangang Road, Huangdao District, Qingdao, 266590  
CHINA

*Abstract:* - In order to analyze the bifurcation and chaos of Superbuck converter in Continuous Current Mode (CCM), a new method of time-frequency diagram based on Wigner-Ville distribution is proposed. The method is used to analyze the variation of the energy component of the output voltage with frequency and time. It reveals that the Superbuck converter exhibits period-1 bifurcation, period-2 bifurcation, period-4 bifurcation and chaos under different reference current. The results of the time-frequency diagram are consistent with the results of the bifurcation diagram, time-domain diagram, phase diagram and Poincare section. It proves that the method can deeply understand the nature of bifurcation and chaos in Superbuck converter, and it provides a new way to analyze the nonlinear phenomena of DC-DC converter.

*Key-Words:* - Superbuck converter, Nonlinear phenomenon, Matlab/Simulink, Wigner-Ville distribution

Received: December 20, 2019. Revised: May 12, 2020. Accepted: June 6, 2020. Published: June 18, 2020

## 1 Introduction

Superbuck converter is a fourth-order circuit composed of simplified boost converter and sepic converter in parallel [1]. Compared with the basic buck, boost, buck-boost converter and other second-order circuits, the Superbuck converter realizes zero ripple input current and continuous output current [2]. And because it can continuously track the maximum power point of the photovoltaic array output and has the characteristics of smaller output voltage ripple, thus it is widely used in photovoltaic power generation, aerospace, electronic vehicles and other fields [3]-[5]. Therefore, many studies on the design and operation mode of the topology of the Superbuck converter have been proposed in recent years, as discussed in [6]-[8]. However, there are little studies on the nonlinear phenomena of Superbuck converters. Therefore, the in-depth analysis of the nonlinear behavior of Superbuck converter is of great significance for improving the characteristics and the control performance of the converter [9]-[11]. In this paper, we will introduce a new way to analyze nonlinear phenomena in CCM mode controlled Superbuck converters [12].

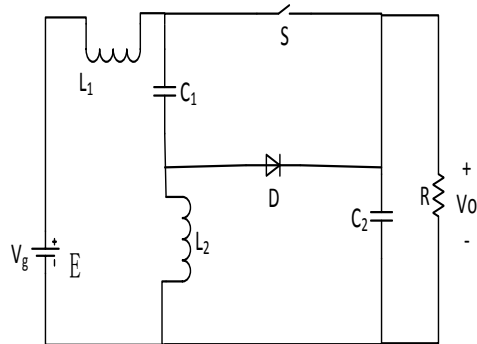
The analytical methods of DC-DC converters include linear and nonlinear analysis [13]. Linear analysis is relatively mature, typical state-space averaging method has been described in [14]. However, the existence of active components such as inductors, capacitors and the strong nonlinearity

of the switching power supply, when the circuit parameters change the output voltage of the converter will also change accordingly. Under certain conditions, the converter will generate bifurcation and may enter a chaotic state, which causes the system to lose stability [15]. The root cause of such complex behaviour has been identified collectively as nonlinearity. The nonlinear analysis methods for DC-DC converters are: phase diagram, bifurcation diagram, Lyapunov index, Poincare map, power spectrum analysis, etc., as discussed in [16]-[18]. Among them, phase plane trajectory analysis and Lyapunov exponent-based analysis are more common [19]-[20]. Using time-frequency analysis to study the nonlinearity of DC/DC converter is still in infancy. Time-frequency analysis method is mainly used to study time-varying non-stationary signal [21]-[22]. Since the output voltage of DC/DC converter is non-stationary signal, it can be applied to the nonlinear analysis of DC/DC converter. Time-frequency analysis can be divided into linear analysis and nonlinear analysis. Short-time Fourier Transform (STFT) is the most widely used linear method. It with fixed resolution and its resolution is low, which cannot take into account both high-frequency information and low-frequency information [23]-[24]. But the Wigner-Ville distribution has high resolution, and it can clearly describe the energy distribution of the signal in the time-frequency plane, so its application is increasing in recent years. The time-frequency

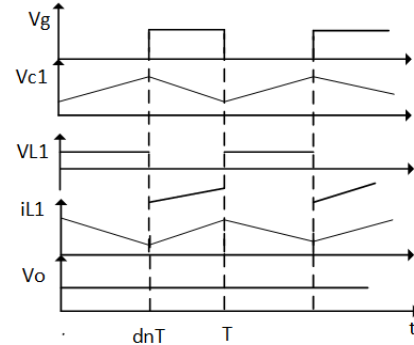
analysis of Wigner-Ville distribution is widely used in lidar, coalmine, etc. The Wigner-Ville distribution is used to process the characteristic guided wave echo signals of the weld [25]. Analyzing the guided wave pattern of each wave packet to effectively identify the defect echo signal. By extracting the structure and defect information of the weld, modal separation and defect recognition are realized [26]. The literature [27] applies the Wigner-Ville distribution to study the frequency, amplitude, and energy distribution characteristics of signals in wide-area measurement systems. Experiments show that the method has strong anti-noise ability and better identification results, and can better reflect the local characteristics of non-stationary signals. However, the time-frequency analysis of Wigner-Ville distribution has little study of the DC/DC converters. In this paper, the time-frequency diagram based on Wigner-Ville distribution is introduced to analyze the nonlinear phenomena of Superbuck converter. Like the classic identification method, the Wigner-Ville distribution can clearly identify the route that the Superbuck converter enters chaos from a stable state.

## 2 Principle and state equation of Superbuck converter

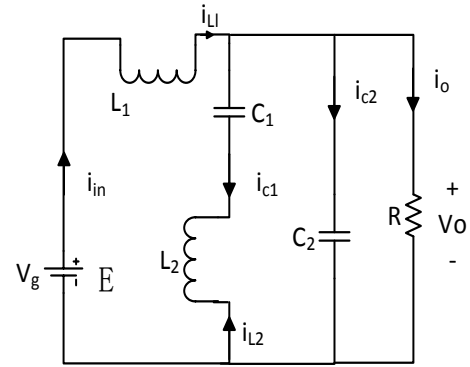
Superbuck is a fourth-order buck converter. Its topology includes: input voltage  $E$ , switch  $S$ , diode  $D$ , inductor  $L_1$ ,  $L_2$ , and capacitors  $C_1$  and  $C_2$ . Fig. 1 shows the Superbuck converter circuit topology and its operating process diagram.



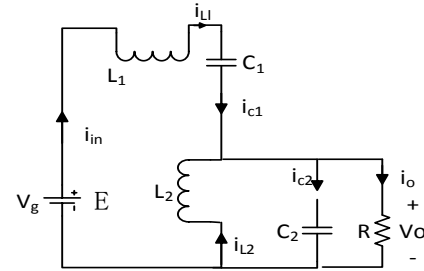
(a) Superbuck topology



(b) Main working waveform



(c) S closed topology



(d) S disconnected topology

Fig. 1 Superbuck converter and its operating process diagram

The Superbuck converter works under CCM:

$$v_o = DE \quad (1)$$

where,  $E$  is the input voltage,  $v_o$  is the output voltage, and  $D$  is the duty cycle of switch  $S$ ,  $0 < D < 1$ . It can be seen from the formula that the Superbuck converter is a buck converter, and the output polarity is the same as the input polarity [28].

Nonlinear components such as capacitors and inductors may make the output voltage and inductor current of the converter unstable, and the output waveform does not work periodically.

Typically, the switch and the diode are turned on and off in a cyclic and complementary manner:

when the switch  $S$  is turned on, the diode  $D$  is reverse biased and it acts as an open circuit. The input voltage  $E$  directly supplies the capacitor  $C_2$  and the load  $R$  through the inductor  $L_1$  and the switch  $S$ , while the capacitor  $C_1$  supplies energy to

the capacitor  $C_2$  and the load through the inductor  $L_2$ . The inductor current  $i_{L1}$  and  $i_{L2}$  rise almost linearly. The current at the switch S is the sum of the inductor current  $i_{L1}$  and  $i_{L2}$ . The output current flows through the load from top to bottom, producing an output voltage that is positive and negative at both ends of R. According to the working principle of the circuit, the KVL and KCL equations are written for the working state when the switch is turned on. State equation can be got:

$$\dot{x} = A_1x + B_1E \quad (2)$$

when the switch S is turned off, the diode D is forward biased and behaves as a short circuit. The input voltage E charges the capacitor  $C_1$  through the inductor  $L_1$ , the inductor  $L_2$  supplies energy to the capacitor  $C_2$  and the load R, the inductor current  $i_{L1}$  and  $i_{L2}$  linearly decrease. Also write the KVL and KCL equations for the state of the switch off. State equation can be got:

$$\dot{x} = A_2x + B_2E \quad (3)$$

where, the state variables  $\dot{x} = [i_{L1} \ i_{L2} \ v_{c1} \ v_{c2}]^T$ ,  $i_{L1}$ ,  $i_{L2}$  are inductor currents,  $v_{c1}$ ,  $v_{c2}$ , are capacitor voltages,  $A_1$ ,  $A_2$ ,  $B_1$ ,  $B_2$  are state matrices, as follows:

$$A_1 = \begin{bmatrix} 0 & 0 & 0 & -\frac{1}{L_1} \\ 0 & 0 & \frac{1}{L_2} & -\frac{1}{L_2} \\ 0 & -\frac{1}{C_1} & 0 & 0 \\ \frac{1}{C_2} & \frac{1}{C_2} & 0 & -\frac{1}{RC_1} \end{bmatrix}$$

$$A_2 = \begin{bmatrix} 0 & 0 & -\frac{1}{L_1} & -\frac{1}{L_1} \\ 0 & 0 & 0 & -\frac{1}{L_2} \\ \frac{1}{C_1} & 0 & 0 & 0 \\ \frac{1}{C_2} & \frac{1}{C_2} & 0 & -\frac{1}{RC_2} \end{bmatrix}$$

$$B_1 = B_2 = \begin{bmatrix} \frac{1}{L_1} \\ 0 \\ 0 \\ 0 \end{bmatrix}$$

where, R,  $L_1$ ,  $L_2$ ,  $C_1$ , and  $C_2$  are the values of the resistance, inductance, and capacitance of the Superbuck converter, respectively.

By introducing the switching function  $\delta$ , the state equations of switch on and off can be combined to obtain a unified expression of the circuit.

$$\dot{x} = (\delta A_1 + (1-\delta)A_2)x + (\delta B_1 + (1-\delta)B_2)E \quad (4)$$

Introducing Laplace transform to formula (4) can get unified expression (5). The formula (5) is the expression of the piecewise switched model.

$$\begin{cases} i_{L1} = \frac{V_{in} - v_o(1-\delta)v_{c1}}{sL_1} \\ i_{L2} = \frac{\delta v_{c1} - v_o}{sL_2} \\ v_{c1} = \frac{(1-\delta)i_{L1} - \delta i_{L2}}{sC_1} \\ v_o = \frac{i_{L1} + i_{L2} - v_o/R}{sC_2} \end{cases} \quad (5)$$

$$\delta = \begin{cases} 0 & \text{switch S is turned on} \\ 1 & \text{switch S is turned off} \end{cases} \quad (6)$$

where,  $1/s$  is the integral factor,  $\delta$  is the switching function,  $v_o = v_{c2}$  is the output voltage of the Superbuck converter.

### 3 Superbuck converter simulation model

To mimic the true behavior of the circuit, the piecewise switched model is used for simulation. According to the unified expansion (5), a current feedback type based on the piecewise switched mode in CCM mode is established. The comparator compares the value of the inductor current  $i_{L1}$  with the value of the reference current  $I_{ref}$ , and then forms a feedback control circuit with the clock pulse to control the closing and opening of the switch S through the S-R flip-flop. Assuming that the switch S is closed at the initial time, the value of inductance current  $i_{L1}$  is less than that of  $I_{ref}$ , the comparator output low level. When the rising edge of clock pulse arrives, the S-R flip-flop will output high level. As long as the value of  $i_{L1}$  is less than the value of  $I_{ref}$ , the comparator will always output low level, and the S-R flip-flop will always maintain high level output. Until  $i_{L1}$  increases to  $I_{ref}$ , the comparator outputs a high level. At this time, the S-R flip-flop is reset, causing the switch S to be turned off, then the inductor current is gradually decreased until the next clock pulse comes and the switch S will be again turned off. According to the operating principle of current feedback type switch and the integral mathematical expression of switching function integral factor in CCM mode (5), the piecewise switched model is built, as shown in Fig. 2.

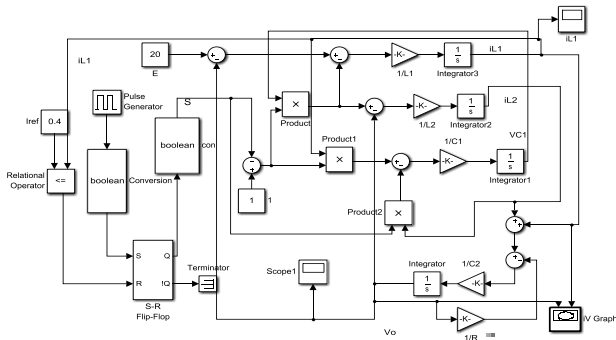


Fig.2 The piecewise switched model of CCM Superbuck converter

The simulation parameters are as follows:

Table 1 Circuit parameter value table

| Circuit parameter           | Reference value |
|-----------------------------|-----------------|
| Inductance $L_1$            | 0.5mH           |
| Inductance $L_2$            | 5mH             |
| Resistance $R$              | 10 $\Omega$     |
| Capacity $C_1$              | 2.2uF           |
| Capacity $C_2$              | 1uF             |
| input voltage $E$           | 20V             |
| Reference current $I_{ref}$ | 0.2A-1.4A       |
| Switching cycle $T$         | 10us            |

### 3 Simulation of Superbuck converter

Taking the reference current  $I_{ref}$  as a bifurcation parameter, the bifurcation diagram of the inductor current  $i_{L1}$  can be obtained by through the piecewise switched model in Simulink, as shown in Fig. 3.

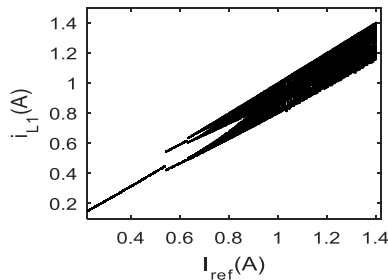


Fig. 3 Superbuck Bifurcation of  $i_{L1}$

From Fig.3, it shows that as the reference current increases, the inductor current  $i_{L1}$  begins to bifurcate and enters a chaotic state.

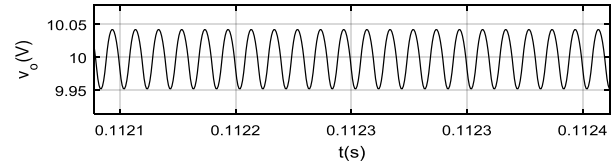
In order to better analyze the bifurcation of the Superbuck converter, this section introduces the Wigner-Ville distribution analysis. For signal  $x(t)$ , the Wigner-Ville distribution is:

$$W(t, f) = \int_{-\infty}^{+\infty} x(t + \frac{\tau}{2}) \cdot x^*(t - \frac{\tau}{2}) e^{-j2\pi f \tau} d\tau \quad (7)$$

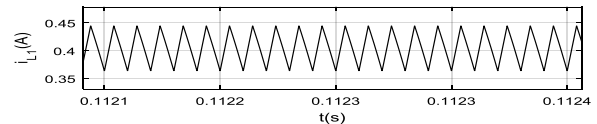
where,  $t$  is a time variable,  $f$  is a frequency variable,  $*$  represents complex conjugate.

By processing the simulation data of the piecewise switched model and writing time-frequency program in the M file in Matlab, the

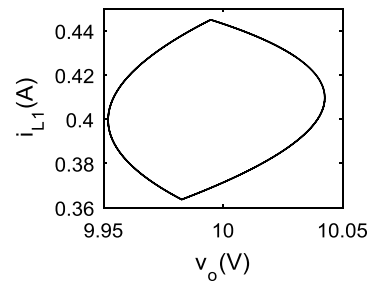
bifurcation parameters  $I_{ref}$  are selected as 0.445A, 0.54A, 0.626A and 1A. The time domain waveform of the inductor current  $i_{L1}$ , the output voltage  $v_o$  and the time-frequency diagram of the Wigner-Ville distribution can be obtained. As shown in Fig. 4- Fig. 7.



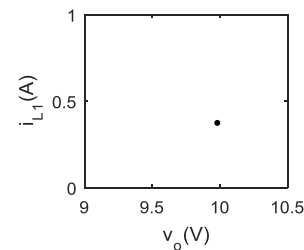
(a) Time domain waveform of output voltage  $v_o$



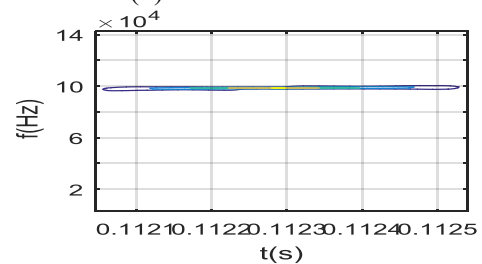
(b) Time domain waveform of inductor current  $i_{L1}$



(c) The phase diagram of  $v_o - i_{L1}$



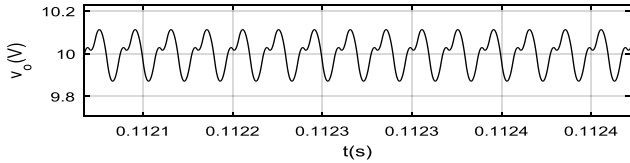
(d) Poincare section



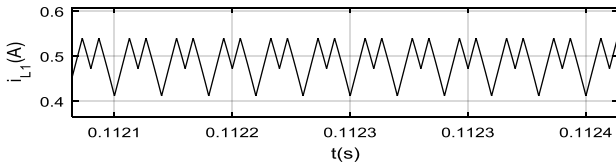
(e) Time-frequency diagram of output voltage  
Fig. 4 Superbuck Converter operates at Period-1 operation ( $I_{ref}=0.445A$ )

We can see that in Fig. 4, when  $I_{ref}=0.445A$ , the circuit operates in stable period-1. The time-domain waveforms are periodic. The output voltage is a steady sine wave and the inductance current is a steady sawtooth wave. The phase diagram is a closed ring formed by a curve. There is only one

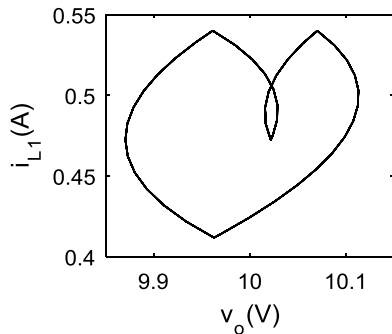
mapping point on the Poincare section. From the time-frequency diagram, the AC power of the output voltage is mainly concentrated near the switching frequency of 100 kHz. Therefore, at this time it can be concluded that the system runs in period-1 operation according to the time-frequency diagram of Wigner-ville distribution. With the increase of the reference current, the circuit becomes unstable.



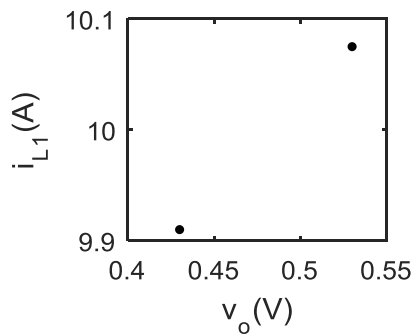
(a) Time domain waveform of output voltage  $v_o$



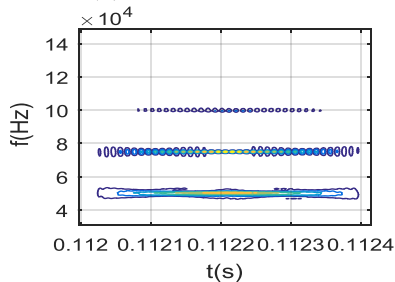
(b) Time domain waveform of inductor current  $i_{L1}$



(c) The phase diagram of  $v_o - i_{L1}$

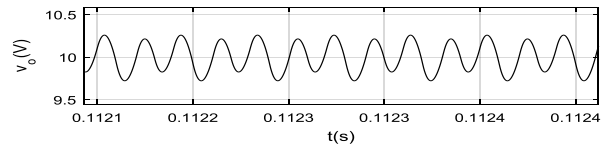


(d) Poincare section

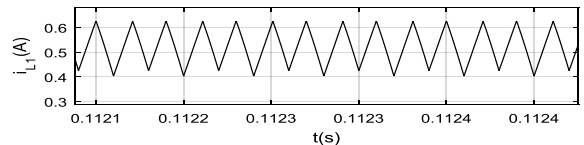


(e) Time-frequency diagram of output voltage  
 Fig. 5 Superbuck Converter operates at Period-2 operation ( $I_{ref}=0.54A$ )

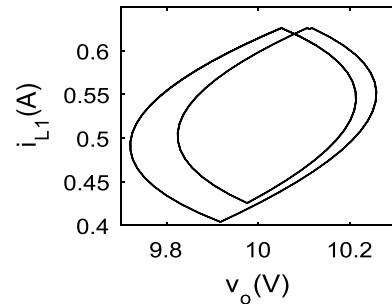
In Fig. 5, when  $I_{ref}=0.54A$ , although the time domain waveform is still periodic, there are two amplitude waves in the output voltage and inductance current. The phase diagram is a closed ring formed by two curves. There are two mapping points on the Poincare section. From the time-frequency diagram of the output voltage, the working frequency of the output voltage is divided into two frequencies: one is the excitation frequency of 100 kHz, the other is the subharmonic frequency of 50 kHz and the interharmonic frequency of 79 kHz. Therefore, it can be judged that when the reference current is 0.54A the Superbuck converter enters period-2.



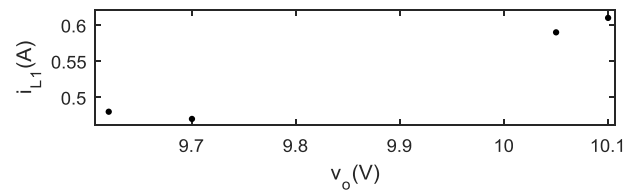
(a) Time domain waveform of output voltage  $v_o$



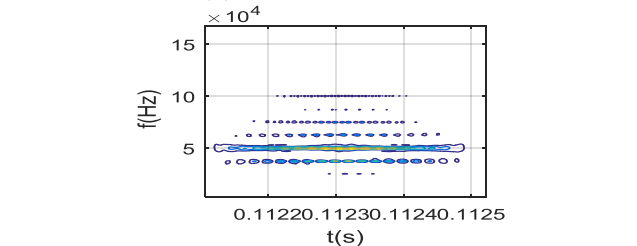
(b) Time domain waveform of inductor current  $i_{L1}$



(c) The phase diagram of  $v_o - i_{L1}$



(d) Poincare section

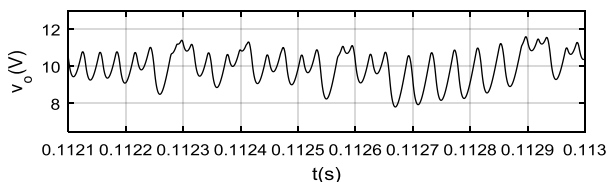


(e) Time-frequency diagram of output voltage

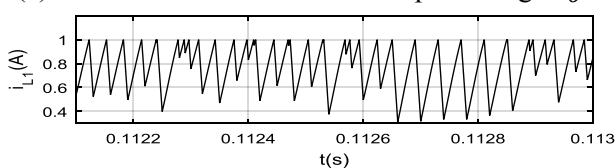
Fig. 6 Superbuck Converter operates at Period-4 operation ( $I_{ref}=0.626A$ )

In Fig. 6, when  $I_{ref}=0.526A$ , the waveforms of inductance current and output voltage show four

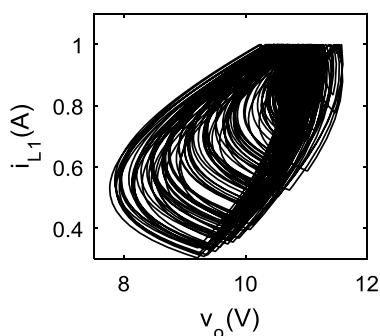
amplitudes. The phase diagram is a closed ring formed by four curves. There are four mapping points on the Poincare section. From the time-frequency diagram of output voltage, it can be seen the base frequency of the time-frequency diagram is about 25 kHz. The main energy of the output voltage is concentrated at 50 kHz, and the interharmonics appear at the moment. It can be considered that the system has entered period-4.



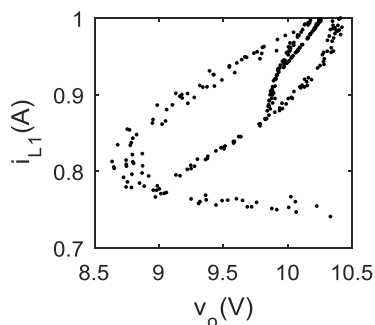
(a) Time domain waveform of output voltage  $v_o$



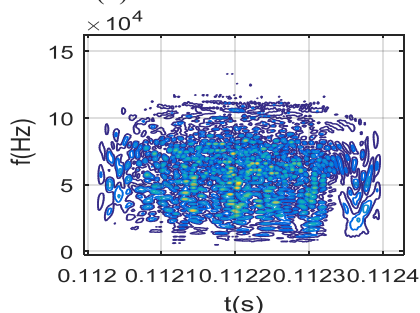
(b) Time domain waveform of inductor current  $i_{L1}$



(c) The phase diagram of  $v_o - i_{L1}$



(d) Poincare section



(e) Time-frequency diagram of output voltage

Fig. 7 Superbuck Converter operates at Chaotic operation ( $I_{ref}=1A$ )

In Fig. 7, when the reference current is increased to 1A, the waveforms of inductance current and output voltage no longer show periodic and the system obviously enters chaos. The phase diagram enters chaotic state. There are countless mapping points in the Poincare section. Energy messy distribution of output voltage in time-frequency diagram. According to the time-frequency diagram it can be seen that the Superbuck converter exhibit chaotic behavior. The AC power of the voltage is significantly increased, most of it is moved to the subharmonic and interharmonic frequencies.

From Fig. 4 to Fig. 7, it shows that the Wigner-Ville distribution results are the same as the bifurcation diagram result. In the non-chaotic state, the waveforms of the inductor current  $i_{L1}$  and the output voltage  $v_o$  are periodic, and their periods are multiplied by the switching period  $T$ . The phase diagram is composed of a finite closed curve, and the mapping points of the Poincare section corresponds to the periodic orbit. The output voltage frequency is distributed over one or several finite frequencies corresponding to the periodic orbits. Superbuck converter in chaos has a non-periodic waveform of the inductor current  $i_{L1}$  and the output voltage  $v_o$ . The phase diagram and the Poincare section present a chaotic state. In order to make the converter operating in steady state, it is necessary to keep its parameters away from the bifurcation point as far as possible. Through the above analysis, it can be seen that the process of Superbuck converter from bifurcation to chaos can be identified by using the time-frequency diagram of Wigner-Ville distribution.

## 4 Conclusion

In this paper, the piecewise switched model of CCM current feedback Superbuck converter is established and a time-frequency diagram analysis method based on Wigner-Ville distribution is proposed to analyze the output voltage energy distribution of Superbuck converter. The Wigner-Ville distribution of single component signal has good time-frequency aggregation. The energy distribution of the signal is at a certain frequency and time range can be visually known by time-frequency diagram, so that the state of the converter can be clearly judged.

By comparing with other recognition methods, we see the time-frequency diagram of the Wigner-Ville energy distribution can be used to identify the process of the Superbuck converter entering chaos from steady state. By description of the operating

dynamics of the Superbuck converter's output voltage provides a new idea for the nonlinear analysis of Superbuck converters. The shortcoming is that there is cross-term interference in the Wigner-Wille distribution, which can be removed in future study.

### Acknowledgments

This work was supported by the Natural Science Foundation of Shandong Province, China, under Grant ZR2018MF005.

### References:

- [1] J. D. Navamani, A. Lavanya and K. Vijayakumar, Modified SEPIC Converter with High Boosting Capability, *Electronics Letters*, Vol.55, No.13, 2019, pp.759-760.
- [2] L. L. Kong, J. Y. Wang, L. Wang and J. J. Zhang, Study on Ripple Suppression Method of High-power High-voltage DC Power Supply, *Chinese Journal of Quantum Electronics*, Vol.35, No.4, 2018, pp.419-423.
- [3] G. S. Zhang, W. J. Lei, Y. Zheng, Y. G. Chen and C. G. Wan, Research on High Efficiency Battery Charge Regulator Based on Superbuck Topology, *Power Supply Technology*, Vol.39, No.9, 2015, pp.1937-1940.
- [4] K. L. Liang, X. Z. Mu and H. Wang, Non-Isolated Three Port Converter Research Based on Zeta and SuperBuck for Aerospace Power Supply, *Transactions of China Electrotechnical Society*, Vol.32, No. S2, 2017, pp.139-147.
- [5] L. Qin, X. Xiao, J. F. Mao, S. J. Xie and M. Hu, ZCS-PWM Superbuck Converter with Reduced Electric Stress for Electric Vehicle DC Charging Spot in Large Parking Lot, *Transactions of China Electrotechnical Society*, Vol.30, No.23, 2015, pp.32-41.
- [6] X. Cheng, H. X. Xue, Y. Wei, H. Yang and C. Zhang, Double Loop Control Strategy Based on Superbuck Converter, *Micromotors*, Vol.50, No.2, 2017, pp.41-44.
- [7] H. L. Pan, H. Y. Guo, J. G. Yue, Z. G. Liu and Z. M. Liao, Design of Control System for Small Signal Model Superbuck Converter, *Science Technology and Engineering*, Vol.15, No.31, 2015, pp.61-66.
- [8] X. L. Yang and J. S. Kong, A Design of Bidirectional Superbuck Converter for Microsatellite, *Power Supply World*, Vol.12, 2015, pp.21-25.
- [9] Z. Chen, Y. Chen and Z. Yan, Simplified Hysteresis Sliding-Mode Control for Superbuck Converter, *IEEE Transactions on Circuits and Systems II: Express Briefs*, 2020, pp.1-1.
- [10] B. Li, J. Wu, L. Hao, M. Shao, R. Zhang and W. Zhao, Anti-Jitter and Refined Power System Transient Stability Assessment Based on Long-Short Term Memory Network, *IEEE Access*, Vol.8, 2020, pp.35231-35244.
- [11] R. Riaza, Homogeneous Models of Nonlinear Circuits, *IEEE Transactions on Circuits and Systems I: Regular Papers*, Vol.67, No.6, 2020, pp.2002-2015.
- [12] C. Bi, Q. Zhang, Y. Xiang and X. S. Feng, Experimental Study of Peak Voltage Feedback Superbuck in Bifurcation and Chaos, *Journal of Electronics & Information Technology*, Vol.35, No.9, 2013, pp.2261-2265.
- [13] H. L. Li, L. H. Wang, X. Ni and R. Zhang, Analysis of Nonlinear Phenomena in Bidirectional DC-DC Converter of DC Uninterruptible Power Supply, *Telecom Power Technology*, Vol.35, No.7, 2018, pp.1-4+18.
- [14] J. Y. Wang, C. Y. Ma, M. Li and C. Zhao, Modeling and Simulation of Single-Phase Power Factor Correction Based on Generalized State Space Average Method, *Science Technology and Engineering*, Vol.18, No. 20, 2018, pp.233-239.
- [15] K. D. Kim, H. M. Lee, S. W. Hong and G. H. Cho, A Noninverting Buck-Boost Converter With State-Based Current Control for Li-ion Battery Management in Mobile Applications, *IEEE Transactions on Industrial Electronics*, Vol.66, No.12, 2019, pp.9623-9627.
- [16] L. Yuan, J. Q. Shen and F. Xiao, Modeling of Current Mode Control Buck-Boost Converter and Simulation of Nonlinear Phenomena. *Journal of Central South University, Science and Technology*, Vol.43, No.2, 2012, pp.972-979.
- [17] G. L. Li, C. Y. Li, X. Y. Chen and X. M. Mu, Study on Period-Doubling Bifurcation Phenomenon in Current-Mode SEPIC Converter, *Acta Physica Sinica*, Vol.61, No.17, 2012, pp.88-96.
- [18] H. B. Lin, Z. B. Gao, Chuijie Yi and Tianran Lin, Simulation Study on Multi-Rate Time-Frequency Analysis of Non-Stationary Signals, *Journal of Shanghai Jiaotong University (Science)*, Vol.23, No.06, 2018, pp.798-802.
- [19] F. Li, X. J. You and Y. Li, Research on State Trajectories and Characteristics of Families of Inductor-Less Converters, *Transactions of China Electrotechnical Society*, Vol.29, No. S1, 2014, pp.242-249.
- [20] H. Wapas, Lu. D. Dah-Chuan and W. D. Xiao, Single-Switch High Step-Up DC-DC Converter With Low and Steady Switch Voltage Stress,

- IEEE Transactions on Industrial Electronics, Vol.66, No.12, 2019, pp.9326-9338.
- [21] G. Z. Cheng, Study on fault diagnosis of main fan in coal mine based on time frequency analysis, *China Energy and Environmental Protection*, Vol.40, No.8, 2018, pp.145-149.
- [22] L. Wang, L. Feng, Y. Q. Su, J. G. Yue, Kernel Entropy-Based Classification Approach for Superbuck Converter Circuit Fault Diagnosis, *IEEE Access*, No.6, 2018, pp.45504-45514.
- [23] H. Ouyang, Q. Li and W. Li, Simulation on Design Based on Superbuck Converter, *2019 6th International Conference on Information Science and Control Engineering (ICISCE)*, Shanghai, China, 2019, pp. 898-902.
- [24] W. Hong and M. Lee, A 7.4-MHz Tri-Mode DC-DC Buck Converter with Load Current Prediction Scheme and Seamless Mode Transition for IoT Applications, *IEEE Transactions on Circuits and Systems I: Regular Papers*.
- [25] Z. Y. Xu, H. Liu, D. Y. Wan, H. Hong, Signal analysis method for weld feature-guided wave based on Wigner-Ville distribution, *China Measurement & Test*, Vol.43, No.09, 2017, pp.29-34.
- [26] P. Jia, T. Q. Zheng and Y. Li, Parameter Design of Damping Networks for the Superbuck Converter, *IEEE Transactions on Power Electronics*, Vol.28, No.8, 2013, pp.3845-3859.
- [27] Y. P. Liu, C. Wang, H. Y. Xia, Application Progress of Time-frequency for Lidar, *Laser & Optoelectronics Progress*, Vol.55, No.12, 2018, pp.68-83.
- [28] S. Teuvo, J. Leppaaho, J. Huusari and L. Nousiainen, Issues on Solar-Generator Interfacing With Current-Fed MPP-Tracking Converters, *IEEE Transactions on Power Electronics*, Vol.25, No.9, 2010, pp.2409-2419.

**Creative Commons Attribution  
License 4.0 (Attribution 4.0  
International , CC BY 4.0)**

This article is published under the terms of the Creative Commons Attribution License 4.0  
[https://creativecommons.org/licenses/by/4.0/deed.en\\_US](https://creativecommons.org/licenses/by/4.0/deed.en_US)